

## Two-Dimensional Frequency Resolved Optomolecular Gating of High-Order Harmonic Generation

A. Ferré,<sup>1</sup> H. Soifer,<sup>2</sup> O. Pedatzur,<sup>2</sup> C. Bourassin-Bouchet,<sup>3</sup> B. D. Bruner,<sup>2</sup> R. Canonge,<sup>1</sup> F. Catoire,<sup>1</sup> D. Descamps,<sup>1</sup> B. Fabre,<sup>1</sup> E. Mével,<sup>1</sup> S. Petit,<sup>1</sup> N. Dudovich,<sup>2</sup> and Y. Mairesse<sup>1</sup>

<sup>1</sup>Université de Bordeaux—CNRS—CEA, CELIA, UMR5107, F33405 Talence, France

<sup>2</sup>Department of Physics of Complex Systems, Weizmann Institute of Science, Rehovot 76100, Israel

<sup>3</sup>Synchrotron SOLEIL, Saint Aubin, BP 34, 91192 Gif-sur-Yvette, France

(Received 16 June 2015; published 2 February 2016)

Probing electronic wave functions of polyatomic molecules is one of the major challenges in high-harmonic spectroscopy. The extremely nonlinear nature of the laser-molecule interaction couples the multiple degrees of freedom of the probed system. We combine two-dimensional control of the electron trajectories and vibrational control of the molecules to disentangle the two main steps in high-harmonic generation—ionization and recombination. We introduce a new measurement scheme, frequency-resolved optomolecular gating, which resolves the temporal amplitude and phase of the harmonic emission from excited molecules. Focusing on the study of vibrational motion in  $N_2O_4$ , we show that such advanced schemes provide a unique insight into the structural and dynamical properties of the underlying mechanism.

DOI: 10.1103/PhysRevLett.116.053002

Recent progress in high-order harmonic generation (HHG) has opened new pathways for resolving the structure and dynamics of electronic wave functions. HHG occurs via a subcycle recollision process: within one optical cycle an electron is removed from the molecule by strong field ionization, accelerated in the continuum and recollides with the parent ion to emit extreme ultraviolet radiation [1,2]. This process is very sensitive to the ionization potential and structure of the contributing orbitals, as well as to possible couplings by the laser field [3–7]. While this sensitivity to multiple parameters makes high-harmonic spectroscopy a promising tool to study ultrafast dynamics [8,9], disentangling the different degrees of freedom encoded in the emission is a major challenge. In this Letter, we present a significant advance by separating the different steps in the probing mechanism and measuring the evolution of the two complex vectorial components of the harmonic emission.

We focus on the study of  $N_2O_4$  molecules, emblematic of the major limitations of HHG spectroscopy. Large vibrational motion can be excited in the electronic ground state of  $N_2O_4$  by stimulative impulsive Raman scattering [10]. This motion induces modulations of the harmonic intensity [11], whose origin remains debated. They were initially attributed to a switch between the ionic states involved in HHG as the bond length changes [11], which would lead to strong changes in the electron recombination dipole moment; this interpretation was later challenged by a study revealing a significant modulation of the ionization yield [12], and by calculations of the modulations of the recombination dipole moments in a single channel picture [13].

The experiments were carried out using the 1 kHz 800 nm Aurore laser system at CELIA which delivers 7 mJ 25 fs pulses. The laser beam is split by a 80%/20% beam splitter. The weakest one (pump beam) is focused by a  $f = 37.5$  cm silver coated spherical mirror at  $\sim 8 \times 10^{13}$  W/cm<sup>2</sup> at the exit of a 100 Hz pulsed valve (General Valve) backed with  $\sim 1$  bar of  $NO_2/N_2O_4$  mixture. The temperature of the valve is 300 K, such that the proportion of  $N_2O_4$  is  $\sim 65\%$ . The time-delayed second pulse probes the vibrationally excited molecules by two-color HHG. A BBO crystal (type I, 100  $\mu$ m thick) generates 400 nm light ( $\sim 5\%$  conversion efficiency) with a polarization direction perpendicular to the 800 nm incident beam. The delay between the 400 and 800 nm pulses is overcompensated by introducing a 1 mm thick calcite plate, and finely controlled by a set of two BK7 wedges of 200  $\mu$ m minimum thickness. The probe is sent to the same mirror as the pump and focused at  $\sim 1.2 \times 10^{14}$  W/cm<sup>2</sup> to produce harmonics. The pump and probe beams are slightly noncollinear ( $\sim 40$  mrad angle). An extreme ultraviolet grating resolves the harmonics spectrally and spatially. They are detected by microchannel plates, a phosphor screen, and a CCD camera. The polarization of the pump pulse is controlled by a zero-order broadband half wave plate. In the following we refer to the parallel configuration when the polarizations of the 800 nm pump beam and 800 nm probe beam are parallel, and to the perpendicular configuration when the two 800 nm beams are orthogonal. The 400 nm polarization is always perpendicular to that of the 800 nm probe beam.

Generating harmonics with two orthogonally polarized laser fields enables decoupling the nuclear and electronic

degrees of freedom by engineering the 2D electron trajectories. By manipulating the relative intensity and delay between the 800 and 400 nm fields we can control the angles of ionization and recollision [14]. Furthermore, due to the symmetry of the interaction, even harmonics are polarized along the second-harmonic field polarization, whereas odd harmonics are polarized along the fundamental 800 nm [14]. This scheme thus enables measuring two components of the harmonic dipole moment simultaneously. So far this approach has been applied to resolve the structure of atomic systems and static molecules. Here we integrate it with the ability to control the nuclear degree of freedom—via the vibrational excitation.

Figure 1 shows the harmonic signal as a function of pump-probe delay for H14 and H15 in two cases: parallel and perpendicular pump-probe configuration. Raman scattering is more efficient for molecules aligned parallel to the pump pulse polarization [11]. The excitation thus induces an effective molecular alignment, with a distribution pointing along the polarization of the pump laser. The parallel configuration enables probing molecules vibrating along the direction of the 800 nm probe field, while the perpendicular configuration measures the response perpendicular to the vibrations. The signal oscillates with a  $T_0 = 130$  fs period, corresponding to the large amplitude N-N vibration of  $N_2O_4$ . Stimulated impulsive Raman scattering calculations, described later in the Letter, show that the molecules are stretched at delays  $T_0/4 + nT_0$ , where  $n$  is an integer. In the parallel case, both even and odd harmonics are maximized at these delays. By contrast, in the perpendicular configuration harmonic 14 shows an opposite behavior: it is maximum when the molecules are compressed. This effect is found to be systematic for all detected harmonics from 13 to 22: even and odd harmonics oscillate in opposite phase in orthogonal configuration. This behavior is robust against modifications of the relative phase between the 800 and 400 nm probe fields, i.e., against variations of the recollision angle.

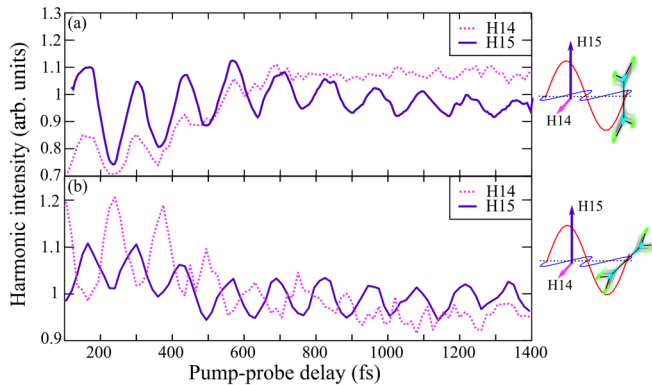


FIG. 1. Intensity of H14 (dots) and H15 (continuous line) as a function of pump-probe delay, in parallel (a) and perpendicular (b) pump-probe configuration.

The harmonic modulation can be decomposed in two terms: modulation of the ionization probability [12], which modifies the amplitude of both even and odd harmonics simultaneously, and modulation of the recombination matrix element, which is specific to each harmonic order. The opposite modulation of even and odd harmonics cannot originate from a modulation of the ionization probability, which affects them in the same way. The two-color HHG thus unambiguously reveals a specific feature of the recollision step, i.e., a modulation of the recombination matrix element. However, this matrix element is complex, and we have to disentangle phase and amplitude effects in the experimental signal in order to elucidate the origin of this modulation.

Phase measurements in high-harmonic spectroscopy have been the subject of intensive research in the past few years. Several schemes, requiring sophisticated instrumentation, have been developed, such as attosecond metrology based on photoelectron spectroscopy [15], transient grating spectroscopy [16], and two-source interferometry [17]. An original approach was initiated by *Vozzi et al.* who used a retrieval algorithm to extract the amplitude and phase from aligned molecules [18]. In the following we show that phase-resolved measurements can indeed be performed without the need of additional experimental devices or molecular alignment, since high-harmonic spectroscopy can be considered as a particular case of frequency resolved optical gating (FROG) [19].

Let us consider the general case of high-harmonic emission from molecules excited by a pump pulse. We will assume that the molecular excitation induces an instantaneous modification of the harmonic emission, such that the field of the  $q$ th harmonic can be written as  $E_q^*(t) = E_q^0(t)G(t-\tau)$ , where  $E_q^0$  is the field in the absence of pump pulse,  $\tau$  the pump-probe delay, and  $G$  the complex modulation introduced by the molecular dynamics. The harmonic spectrum then reads  $S_q(\omega, \tau) = |\int E_q^0(t)G(t-\tau)e^{-i\omega t} dt|^2$ . This equation is characteristic of a FROG measurement. The molecular dynamics act as an amplitude and phase gate, which temporally modulates the harmonic emission. Iterative algorithms, such as the Principle Component Generalized Projections Algorithm (PCGPA)[20], can be used to retrieve the amplitude and phase of both  $E_q^0(t)$  and  $G(t)$ .

To illustrate the influence of the molecular gate on the harmonic spectrum, we simulated the spectrograms associated to a few simple cases. We assume that  $E_q^0$  has a Gaussian temporal profile (15 fs FWHM) and a quadratic temporal phase, characteristic of the intrinsic negative chirp of HHG [21,22]. The molecular gate is a sinusoidal function with 130 fs period, both in amplitude and phase. Figure 2(a) shows the evolution of the spectrum of one harmonic when the molecular gate is a pure amplitude gate (20% modulation depth in intensity). The different spectral components of the harmonic are maximized for different

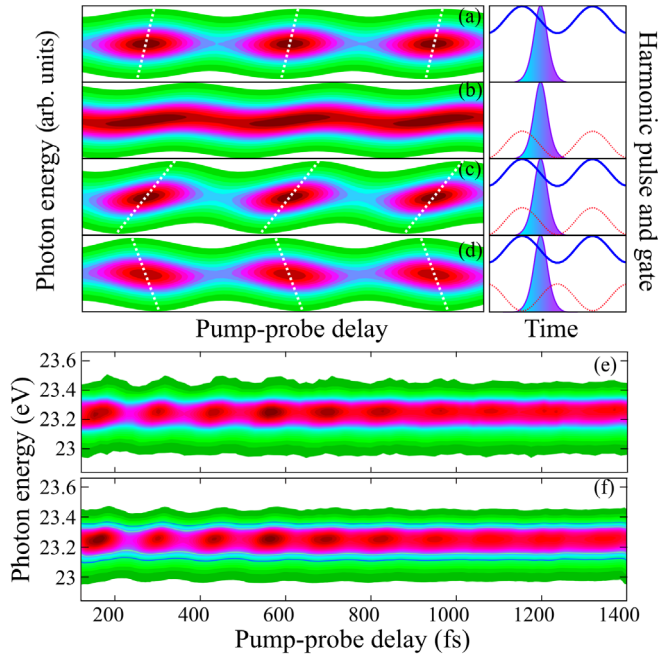


FIG. 2. Simulated FROMAGE traces in simple cases: pure amplitude gate [(a), modulation depth 20% in intensity], pure phase gate [(b), modulation depth 1 rad], combined amplitude and phase gate, oscillating in phase (c) and out of phase (d). Measured (e) and retrieved (f) FROMAGE trace for H15, parallel configuration.

pump-probe delays, which is the signature of the chirp of the harmonic emission. Figure 2(b) shows the effect of a pure phase gate (1 rad deep). The harmonic spectrum shifts periodically. This situation is very similar to a FROGCRAB measurement, in which a sinusoidal femtosecond oscillating phase gate is used to measure an attosecond pulse [23]. Figures 2(c)–2(d) show the spectrograms obtained combining a phase and amplitude gate, which oscillate in phase (c) or out of phase (d). Interestingly, the shape of these spectrograms are qualitatively very different, confirming that spectrally resolved harmonic emission is very sensitive to the details of the molecular modulations.

Applying a PCGPA to the spectrograms shown in Figs. 2(a)–2(d) provides excellent reconstructions of the molecular gate and harmonic pulse within a few hundred iterations. We have performed systematic studies for various parameters, which show that there could be significant errors in the reconstruction, in particular in the case of weak phase modulations. This is indeed no surprise: the variations of the harmonic spectrum induced by the molecular gate are too weak to properly encode the harmonic pulse temporal profile. In that case, blind-FROG is not appropriate and a better strategy to retrieve the molecular gate is to assume that the unperturbed harmonic field  $E_q^0$  is known. This situation corresponds to a referenced cross-correlation FROG (XFROG) in optical pulse characterization [19]. Using this approach, our simulations show that molecular gates with intensity modulations as

low as 1% and phase modulations as low as 100 mrad can be very well reconstructed. We have also conducted a study as a function of the gate period, and found that slow modulations (with a period exceeding 220 fs for a 15 fs harmonic pulse) are not properly reconstructed, because the gate is too slow to properly modulate the signal and encode the FROG information. By contrast, modulations of a period similar to the pulse duration (10 fs) can be retrieved, because they produce spectral modifications that are decoded by the algorithm. This systematic study shows that frequency-resolved optomolecular gating (FROMAGE) will be applicable to a large range of molecular systems and dynamics.

Figure 2(e) shows the experimental spectrogram of harmonic 15, parallel case. The oscillations of the different spectral components of the harmonic are clearly shifted, the blue edge being maximized for later delays than the red edge. We applied an XFROG PCGPA to the experimental data, in which we injected the unperturbed field  $E_q^0$  obtained by Fourier transforming the unperturbed harmonic spectrum (pump off) with a quadratic phase corresponding to a negative chirp of the emission. We varied this chirp to change the harmonic pulse duration between 9 and 18 fs FWHM, which is a reasonable range considering the 30 fs generating pulses [22]. In each case the algorithm converges in a few hundreds of iterations, leading to an excellent agreement between reconstructed [Fig. 2(f)] and experimental [Fig. 2(e)] traces.

Figure 3 shows the retrieved molecular gate for harmonic 14 and 15, parallel and perpendicular configurations. The change in the injected harmonic pulse duration only induces weak modifications of the retrieved gate, which are represented by the line thickness. For harmonic 15 the oscillations of both intensity and phase are stronger in the parallel than in the perpendicular case: from 30% to 10% depth for the intensity, and from  $\sim 400$  to 100 mrad depth for the phase. In both cases the H15 intensity and phase are maximized at the outer turning point of the vibrational wave packet motion. Harmonic 14 shows a more complex behavior. The modulations are more pronounced in the perpendicular case, reaching 30% in intensity and 200 mrad in phase. Remarkably, the modulations of the harmonic intensity and phase are not synchronized [Fig. 3(b)]: the phase reaches its maxima around 45 fs before the intensity. In addition to these fast oscillations, the harmonic amplitude and phase show a continuous increase over the first hundreds of femtoseconds in the parallel case [Fig. 3(a)]. This increase does not appear in the perpendicular configuration [Fig. 3(b)].

The FROMAGE analysis is only valid as long as the harmonic field can be written as the product of an unperturbed signal and a delayed gate. A recent theoretical study has pointed out that the intense probe pulse could induce significant perturbation of the molecular dynamics [13], challenging this hypothesis: the influence of the probe

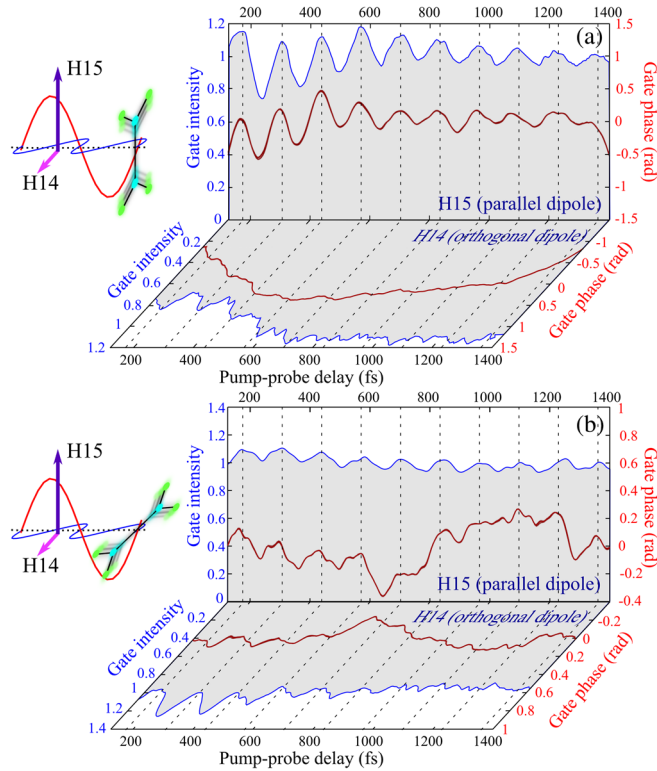


FIG. 3. Reconstructed intensity and phase of the gate for harmonic 14 and 15 in parallel (a) and perpendicular (b) configuration.

pulse would need to be invariant with pump-probe delay for the retrieval procedure to be applicable. To evaluate the validity of this hypothesis, we have performed time-dependent Schrödinger equation vibrational wave packet calculations in a one dimensional model [24]. The fundamental potential energy curve  $V(R)$  of  $N_2O_4$  was calculated using MOLPRO as a function of the distance  $R$  between the  $NO_2$  monomers. The nuclear wave function was obtained by resolving the nuclear time-dependent Schrödinger equation, taking into account the polarizability along the N-N axis calculated for each  $R$ .

Figure 4(a) shows the dynamics of the center of the nuclear wave packet excited by a 29 fs pump pulse of  $8 \times 10^{13}$  W/cm<sup>2</sup> intensity (black curve). The wave packet oscillates with a period of 130 fs between 1.65 and 1.95 Å. The effect of the probe pulse is calculated by adding a second laser pulse (29 fs,  $2 \times 10^{14}$  W/cm<sup>2</sup>) to the simulation. The evolution of the wave packet center during this pulse is very different from the unperturbed case. We have repeated this calculation for various pump-probe delays and show the corresponding wave packet centers in different colors in Fig. 4(a). The effect of the probe pulse is dramatic: it systematically stretches the molecules with respect to the unperturbed case. In order to estimate the influence of the probe pulse on the molecular gate, we calculate the difference between the perturbed and unperturbed wave packet motions [dashed lines in Fig. 4(a)]. The probe-induced wave packet deviation is roughly linear, with a

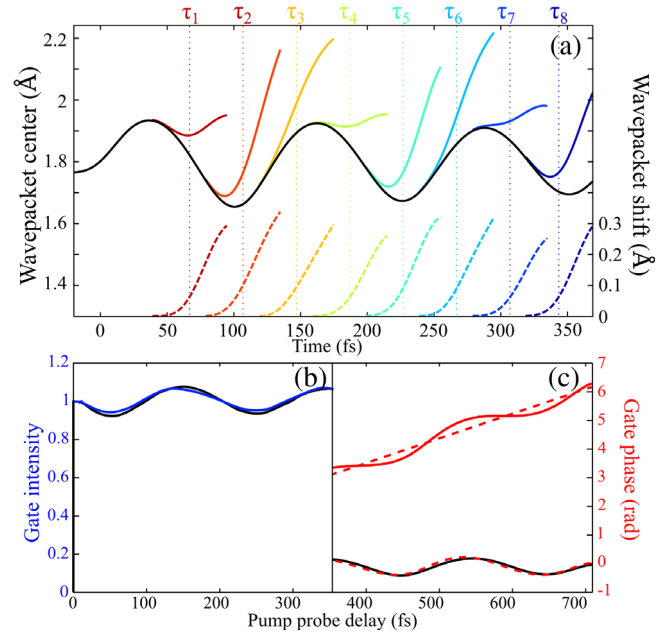


FIG. 4. Effect of the probe pulse on the vibrational wave packet. (a) Wave packet center after a 29 fs pump pulse at  $8 \times 10^{13}$  W/cm<sup>2</sup>, centered around time 0 (black). The different color curves show the evolution when a second 29 fs,  $2 \times 10^{14}$  W/cm<sup>2</sup> probe pulse is applied at increasing pump-probe delays  $\tau_i$ . The dashed lines represent the difference between the wave packet dynamics with and without the probe pulse effect, for each delay. (b) Retrieved gate intensity from a FROMAGE trace neglecting the perturbation by the probe (black), and taking it into account (blue). (c) Retrieved gate phase, without (black) and with (red) probe perturbation. The perturbed phase can be decomposed as the sum of a linear and oscillating term (dashed red curves).

similar slope for all pump probe delays. We have calculated the spectrograms obtained with the perturbed gate and compared the retrieval to the unperturbed case [Figs. 4(b)–4(c)]. Besides a slight modification of the shape of the gate intensity, the main effect of the perturbation is to add a linear term to the gate phase. We can thus consider the probe to induce an additional delay-independent quasilinear stretching of the molecule, which can be retrieved by PCGPA.

How does this analysis relate to the experimental results? The probe pulse is expected to contribute to the wave packet excitation only in the parallel configuration. Remarkably, it is in this configuration that a large, slow increase of the harmonic phase is found over the first few hundreds femtoseconds. This increase is similar to the linear behavior of the reconstructed gate phase, and is the signature of the additional quasilinear stretching of the molecule during the harmonic generation process. FROMAGE is thus able to provide a unique insight into the dynamics induced by the probe pulse by decoding them from the variations of the shape of the harmonic spectrum. The lower slope of the experimental phase ( $\sim 3.5$  mrad/fs)

compared to the theoretical one (8.6 mrad/fs) suggests that the distortions induced by the probe pulse are weaker than expected from theory. This is probably due to the lower value of the laser intensity, and to averaging over alignment angles which lowers the contrast of the response.

While previous experiments in  $N_2O_4$  were only detecting the total harmonic intensity, our measurements provide the phase and amplitude evolution of the parallel and perpendicular components of the harmonic dipole moment modulations. This constitutes an important advance for high-harmonic spectroscopy. The most striking result is that the amplitude of the orthogonal dipole moment is maximized at the inner turning point of the wave packet motion when pump and probe are perpendicular. This could be due to the variation of the recombination matrix elements with bond length, in a single channel picture. Alternatively, this could be the signature of the participation of the  $B_{2g}$  ionic state in the generation process. The contribution of this state is expected to be maximum at low internuclear distance and thus higher in the perpendicular configuration, where the probe pulse does not induce molecular stretching. Furthermore, the ionization probability to the  $B_{2g}$  states shows a local maximum for perpendicular molecules [12], which could favor it. The complete mapping of the vectorial complex properties of the harmonics performed here will enable a much clearer identification of the influence of multiple channels when compared to theoretical calculations.

In conclusion, by combining attosecond scale engineering of the recolliding electron with vibrational excitation we have decoupled ionization and recollision in HHG. Furthermore, we have shown that high-harmonic spectroscopy experiments can be interpreted as a particular case of FROG, providing a direct access to phase and amplitude modulations induced by the molecular dynamics. The combination of these two techniques can be generalized to a broad range of studies of polyatomic molecules in strong fields—where strong coupling between the electronic and nuclear degrees of freedom on both the attosecond and femtosecond time scale is expected to be observed.

We thank R. Bouillaud and L. Merzeau for technical assistance, E. Constant for providing key apparatus used in the experiment, and V. Blanchet, J. Mikosch, S. Patchkovskii, and A. Stolow for fruitful discussion. We acknowledge financial support of the Conseil Regional d'Aquitaine (20091304003 ATTOMOL and COLA 2 No. 2.1.3-09010502), the European Union (LASERLAB-EUROPE II 228334 and LASERLAB-EUROPE 284464), and the French Agence Nationale pour la Recherche (ANR-14-CE32-0014 MISFITS). N. D. acknowledges the Minerva Foundation, the Israeli Science Foundation, the Israeli Centers of Research Excellence program, the Crown photonics Center and the European Research Council Starting Research Grant MIDAS.

- [1] J. L. Krause, K. J. Schafer, and K. C. Kulander, *Phys. Rev. Lett.* **68**, 3535 (1992).
- [2] P. B. Corkum, *Phys. Rev. Lett.* **71**, 1994 (1993).
- [3] J. Itatani, J. Levesque, D. Zeidler, H. Niikura, H. Pepin, J. C. Kieffer, P. B. Corkum, and D. M. Villeneuve, *Nature (London)* **432**, 867 (2004).
- [4] S. Baker, J. S. Robinson, C. A. Haworth, H. Teng, R. A. Smith, C. C. Chirila, M. Lein, J. W. G. Tisch, and J. P. Marangos, *Science* **312**, 424 (2006).
- [5] O. Smirnova, S. Patchkovskii, Y. Mairesse, N. Dudovich, and M. Y. Ivanov, *Proc. Natl. Acad. Sci. U.S.A.* **106**, 16556 (2009).
- [6] S. Haessler, J. Caillat, W. Boutu, C. Giovanetti-Teixeira, T. Ruchon, T. Auguste, Z. Diveki, P. Breger, A. Maquet, B. Carré *et al.*, *Nat. Phys.* **6**, 200 (2010).
- [7] Y. Mairesse, J. Higué, N. Dudovich, D. Shafir, B. Fabre, E. Mével, E. Constant, S. Patchkovskii, Z. Walters, M. Y. Ivanov *et al.*, *Phys. Rev. Lett.* **104**, 213601 (2010).
- [8] W. Li, X. Zhou, R. Lock, S. Patchkovskii, A. Stolow, H. C. Kapteyn, and M. M. Murnane, *Science* **322**, 1207 (2008).
- [9] H. J. Wörner, J. B. Bertrand, B. Fabre, J. Higué, H. Ruf, A. Dubrouil, S. Patchkovskii, M. Spanner, Y. Mairesse, V. Blanchet *et al.*, *Science* **334**, 208 (2011).
- [10] I. Pastirk, M. Comstock, and M. Dantus, *Chem. Phys. Lett.* **349**, 71 (2001).
- [11] W. Li, X. Zhou, R. Lock, S. Patchkovskii, A. Stolow, H. Kapteyn, and M. Murnane, *Science* **322**, 1207 (2008).
- [12] M. Spanner, J. Mikosch, A. E. Boguslavskiy, M. M. Murnane, A. Stolow, and S. Patchkovskii, *Phys. Rev. A* **85**, 033426 (2012).
- [13] A.-T. Le, T. Morishita, R. R. Lucchese, and C. D. Lin, *Phys. Rev. Lett.* **109**, 203004 (2012).
- [14] D. Shafir, Y. Mairesse, D. M. Villeneuve, P. B. Corkum, and N. Dudovich, *Nat. Phys.* **5**, 412 (2009).
- [15] W. Boutu, S. Haessler, H. Merdji, P. Breger, G. Waters, M. Stankiewicz, L. J. Frasinski, R. Taieb, J. Caillat, A. Maquet *et al.*, *Nat. Phys.* **4**, 545 (2008).
- [16] Y. Mairesse, N. Dudovich, D. Zeidler, M. Spanner, D. Villeneuve, and P. Corkum, *J. Phys. B* **43**, 065401 (2010).
- [17] O. Smirnova, Y. Mairesse, S. Patchkovskii, N. Dudovich, D. Villeneuve, P. Corkum, and M. Y. Ivanov, *Nature (London)* **460**, 972 (2009).
- [18] C. Vozzi, M. Negro, F. Calegari, G. Sansone, M. Nisoli, S. De Silvestri, and S. Stagira, *Nat. Phys.* **7**, 822 (2011).
- [19] R. Trebino, *Frequency-Resolved Optical Gating* (Kluwer Academic, Dordrecht, 2000).
- [20] D. Kane, *IEEE J. Quantum Electron.* **35**, 421 (1999).
- [21] J. Mauritsson, P. Johnsson, R. López-Martens, K. Varjú, W. Kornelis, J. Biegert, U. Keller, M. Gaarde, K. Schafer, and A. L'Huillier, *Phys. Rev. A* **70**, 021801 (2004).
- [22] Y. Mairesse, O. Gobert, P. Breger, H. Merdji, P. Meynadier, P. Monchicourt, M. Perdrix, P. Salières, and B. Carré, *Phys. Rev. Lett.* **94**, 173903 (2005).
- [23] Y. Mairesse and F. Quéré, *Phys. Rev. A* **71**, 011401 (2005).
- [24] F. Catoire and H. Bachau, *J. Phys. B* **47**, 124028 (2014).